

# MODULAR ORGANIZATION OF FREQUENCY INTEGRATION IN PRIMARY AUDITORY CORTEX

---

Christoph E. Schreiner,<sup>1</sup> Heather L. Read,<sup>1</sup>  
and Mitchell L. Sutter<sup>2</sup>

<sup>1</sup>*Coleman Memorial Laboratory, W.M. Keck Center for Integrative Neuroscience, University of California, San Francisco, California 94143–0732; e-mail: chris@phy.ucsf.edu, blondie@phy.ucsf.edu;* <sup>2</sup>*Center for Neuroscience, and Section of Neurobiology, Physiology and Behavior, University of California, Davis, California 95616; e-mail: mlsutter@ucdavis.edu*

**Key Words** audition, spectral processing, critical band, topography, physiology, neuroanatomy

■ **Abstract** Two fundamental aspects of frequency analysis shape the functional organization of primary auditory cortex. For one, the decomposition of complex sounds into different frequency components is reflected in the tonotopic organization of auditory cortical fields. Second, recent findings suggest that this decomposition is carried out in parallel for a wide range of frequency resolutions by neurons with frequency receptive fields of different sizes (bandwidths). A systematic representation of the range of frequency resolution and, equivalently, spectral integration shapes the functional organization of the iso-frequency domain. Distinct subregions, or “modules,” along the iso-frequency domain can be demonstrated with various measures of spectral integration, including pure-tone tuning curves, noise masking, and electrical cochlear stimulation. This modularity in the representation of spectral integration is expressed by intrinsic cortical connections. This organization has implications for our understanding of psychophysical spectral integration measures such as the critical band and general cortical coding strategies.

## INTRODUCTION

A fundamental property of hearing is the decomposition of complex sounds into perceptually distinct frequency components (Fletcher 1940, Scharf 1970, Patterson 1974). The ability to discriminate one frequency component from another varies from species to species, apparently reflecting the frequency resolution or filtering properties of auditory sensory receptors and neurons of the species (e.g. Fletcher 1940, Helmholtz 1963, Scharf 1970, Pickles 1975, Nienhuys & Clark

1979, Ehret 1976, Moore 1997). Thus, each receptor on the cochlea and each centrally located auditory neuron responds only to a limited range of frequencies, defined as the frequency filter bandwidth, and can distinguish or “resolve” these frequencies from those outside its range. At the same time, frequency components that fall inside the filter bandwidth cannot be distinguished from each other, and their sound energy is summed for further processing, also known as spectral integration. This behavioral ability to resolve and integrate frequencies can be quantified in a variety of manners but classically is assessed by psychophysically determining the frequency range of a noise that masks or interferes with the detection of a tone positioned at the center frequency of the noise. This psychophysical “critical bandwidth” or “critical band” increases systematically as a function of the center frequency of the noise and in humans is approximately one third of an octave wide (Moore 1997, Scharf 1970). Psychophysically derived critical bandwidths are essentially constant across a wide range of sound intensities. The association of critical bands with many psychoacoustical properties (see Moore 1997, Plomp & Levelt 1965, Plomp 1975, Zwicker et al 1957) have led to an interpretation that auditory information is processed in parallel by separate frequency “channels.” Consequently, the critical band concept reflects in many ways the spectral decomposition of sounds as well as general psychophysical limits for frequency resolution and, conversely, frequency integration.

Not all perceptual properties, however, adhere to the integration limits defined by critical band measures. Several psychophysical phenomena have been demonstrated that require information processing across a frequency range well beyond that of a single critical band (e.g. Hall et al 1984, O’Connor & Sutter 1999). These phenomena led to the realization that sound decomposition can occur at different frequency resolutions, including integration across critical bands. Consequently, critical-band as well as noncritical-band mechanisms of spectral integration must be involved in the analysis of complex sounds (for review see Scharf 1970, Bregman 1990, Moore 1997).

How are these different processing principles reflected in the functional and anatomical organization of the auditory system and, in particular, the primary auditory cortex (AI)? Given the many different stations from sensory epithelium to cerebrum within the auditory system, it is difficult to relate psychophysical properties to specific physiological mechanisms. Neuronal representation of information can be expressed at many different levels of the auditory system and in many different codes. This situation is further complicated because even fundamental psychophysical measures, such as the shape and bandwidth of auditory filters, depend on which signals and test paradigms are used to derive them (e.g. Moore 1997, Plomp 1975). The psychophysical results indicate that the auditory system can analyze sounds with filters of different bandwidths. The processing of sensory information through various filters of different widths is referred to as multiresolution analysis and has been utilized in spatial vision (Graham 1989). Physiologically at the level of AI, functional maps (i.e. topographic cortical representations) of single-unit responses indicate that the auditory system processes

information through filters of different bandwidths and, therefore, may perform a multiresolution analysis.

Because subcortical processing contributes to the functional properties and topographical maps in AI, we begin the considerations of central auditory spectral integration behavior with a brief survey of potential substrates of critical-band behavior along the auditory pathway.

### **Auditory Brainstem**

The auditory nerve and large parts of the ascending auditory pathway maintain a frequency organization that is highly compatible with the notion of a bank of bandpass filters. The source of this organization is the frequency decomposition of incoming auditory information performed by the auditory receptor surface, the basilar membrane. This frequency analysis is directly reflected in the frequency response of auditory nerve fibers (Kiang et al 1967, Kiang & Moxon 1974, Javel 1994, Liberman 1978). For a given center frequency, the bandwidth of auditory nerve fibers is uniform (Rhode & Smith 1985), and at certain stimulus intensities there is a close agreement between the bandwidth of auditory nerve fibers and psychophysically determined bandwidth of critical bands (Evans et al 1992). However, the physiologically determined bandwidth of auditory nerve fibers is not unequivocally matched to psychophysical auditory filters (see Ehret 1995). In particular, the bandwidth of auditory nerve fibers—and many neurons in the cochlear nucleus—is strongly dependent on sound intensity (Ehret & Moffat 1984, Ehret 1995). This is in direct contrast to the relatively intensity-tolerant bandwidth of psychophysically measured critical bands.

### **Auditory Midbrain**

A substantial number of neurons in the auditory midbrain have acquired a frequency integration/resolution behavior that is closely related to the frequency resolution of auditory perception. Many neurons in the central nucleus of the inferior colliculus (ICC) bear a close relationship to psychophysical critical bands when explored with similar signal paradigms (Ehret & Merzenich 1985, 1988). In particular, a large subset of ICC neurons shows a frequency dependence of their bandwidths similar to that of psychophysics. The bandwidth of this subset of ICC neurons is relatively independent of sound intensity (intensity tolerant) like that of the psychophysical critical bandwidth.

Several anatomic and physiologic properties of the ICC appear to support spectral integration within the frequency range of the critical band. A given cochlear frequency band is represented in ICC as a two-dimensional plane or lamina (Merzenich & Reid 1974, Semple & Aitkin 1979). The majority of neurons in ICC have a disc-shaped dendritic configuration that restricts their integrative or synaptic inputs to a single iso-frequency lamina (Oliver & Morest 1984, Shneiderman & Oliver 1989). A small gradient of frequency actually exists within each

iso-frequency lamina, yielding a range of frequencies similar to the limited range of frequencies within a psychophysical critical band (Schreiner & Langner 1997).

The properties of ICC discussed thus far are all consistent with spectral integration within a critical band; however, several features of ICC neurons suggest a parallel means of integrating beyond the range of the psychophysical critical band. Many ICC neurons have frequency bandwidths that are broader than the corresponding psychophysical critical band. Such properties might be predicted given that there are perceptual phenomena that indicate spectral integration outside the critical band (see Moore 1997, Hall et al 1984, O'Connor & Sutter 1999). Indeed, there appears to be a continuous gradient for bandwidth of pure-tone tuning curves that is arranged topographically on the surface of each iso-frequency lamina of ICC (Schreiner & Langner 1988a,b). Accordingly, broad-bandwidth neurons are located more peripherally on the iso-frequency laminae, and narrow-bandwidth neurons are located more centrally on the laminae. The topographic bandwidth gradient observed in ICC is also evident in the thalamocortical system. However, it is conceivable that many of the spectral integration properties of auditory perception are already accounted for at the level of ICC.

### Thalamo-Cortical System

The spectral integration properties of more centrally located neurons, those in the medial geniculate body and the AI, can be expected to reflect the properties of ICC neurons. Although neurons in the medial geniculate body have not been explicitly studied with psychophysically appropriate critical-band stimuli, the range of bandwidths for pure-tone receptive fields (RFs) has been found to be large (Katsuki et al 1959, Aitkin & Webster 1972, Aitkin 1973, Aitkin & Prain 1974, Calford & Webster 1981, Calford et al 1983, Suga 1995, Suga et al 1997). The topographic gradient of pure-tone bandwidths observed in ICC is apparently transformed into a caudal-to-rostral narrow-to-broad bandwidth gradient in the thalamus (Rodrigues-Dagaeff et al 1989). The relationship of these RFs to critical-band or noncritical-band behavior remains unresolved.

The current understanding of the spectral integration properties of neurons across AI is more advanced and is summarized in the following sections. Evidence has been obtained for parallel pathways expressing different spectral integration properties. The nonuniform spatial distribution of neurons across the cortical surface with and without critical-band behavior serves as a basis for discussion of general organizational principles of AI and their role in the processing of complex sounds.

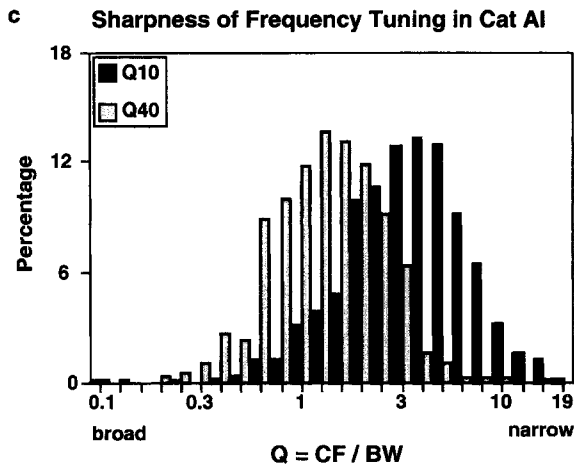
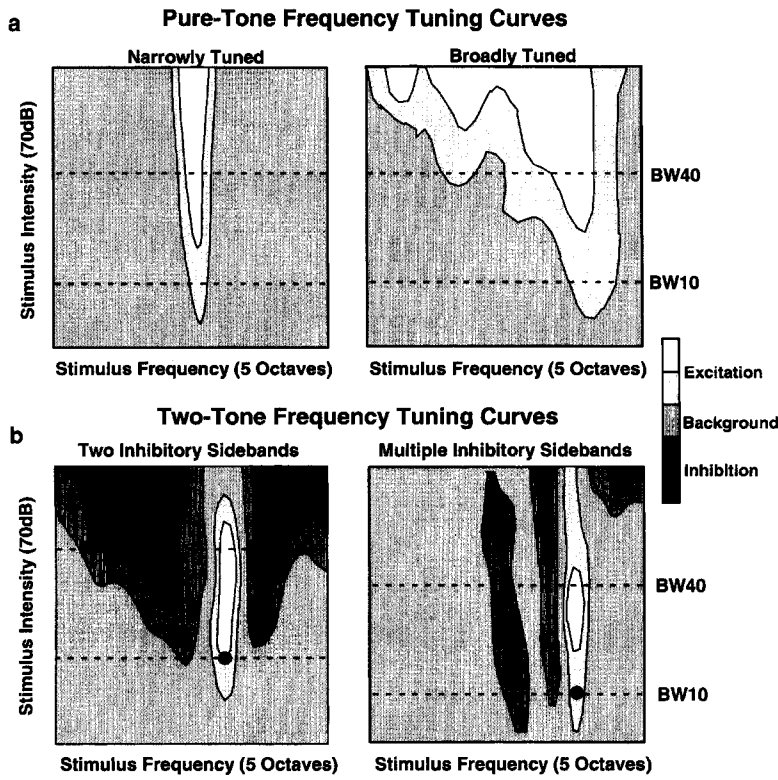
## PHYSIOLOGY OF SPECTRAL INTEGRATION IN PRIMARY AUDITORY CORTEX

### Spectral Integration Measures of Cortical Neurons Derived from Pure Tones Vary Across Primary Auditory Cortex

Studies of sensory cortex have demonstrated that many functional properties of neurons are spatially organized on the cortical surface. This includes topographic gradients of response parameters and circumscribed clusters or patches of neurons with similar RF attributes. These general principles of cortical organization require a fine-grained analysis of response properties across cortical space in order to observe the full range and layout of functional processing.

Spatial mapping of frequency selectivity, excitatory bandwidth, and intensity-dependent response properties has revealed multiple axes of spectral processing across the surface of AI. The tonotopic or "spectral decomposition" axis consists of a single gradient of preferred or characteristic frequency (CF) and has been observed in AI of every mammalian species studied to date (e.g. Merzenich & Schreiner 1992). The tonotopic axis is one dimensional, like the sensory epithelium of the cochlea, and in this respect differs from the two-dimensional retinotopic or somatotopic axes observed in primary visual and somatosensory cortex. A second spectral processing axis has now been demonstrated in AI of several mammalian species, such as cats, monkeys, and ferrets. This second axis is oriented orthogonal to the tonotopic axis and is characterized by multiple gradients of excitatory bandwidth, temporal integration properties, and intensity-dependent coding (Recanzone et al 1999; Phillips et al 1994; He et al 1997, 1998; Heil et al 1992, 1994; Clarey et al 1994; Mendelson et al 1993, 1997; Sutter & Schreiner 1991, 1995; Schreiner & Sutter 1992; Schreiner et al 1992; Schreiner & Mendelson 1990; Shamma et al 1993; Versnel et al 1995). For simplicity, we refer to the first axis as the tonotopic axis and the second axis as the iso-frequency axis. As yet, there is no known integration axis in V1 or S1 that corresponds to the intensity-dependent spectro-temporal integration axis in AI. If such a functional axis exists in the visual system, it has to be embedded in the two-dimensional retinotopic space.

***Single-Peaked Tuning Curves*** Excitatory bandwidths of neurons have generally been assessed by varying pure-tone stimuli over a large range of frequencies and intensities (Figure 1a). For most cortical neurons this results in a single, circumscribed frequency/intensity region of elevated activity. The difference in upper and lower frequency limits of the excitatory region serve as a measure of excitatory bandwidth. Excitatory bandwidth can be expressed either as quality factor ( $Q = \text{CF}/\text{linear bandwidth}$ ) or as logarithmic bandwidth ( $BW$ , expressed in octaves). The range of  $Q$  and  $BW$  values across AI spans approximately 1 to 1.5 orders of magnitude for single and for multiunit responses (Figure 1c). This means that the range of potential spectral integration can be as narrow as one

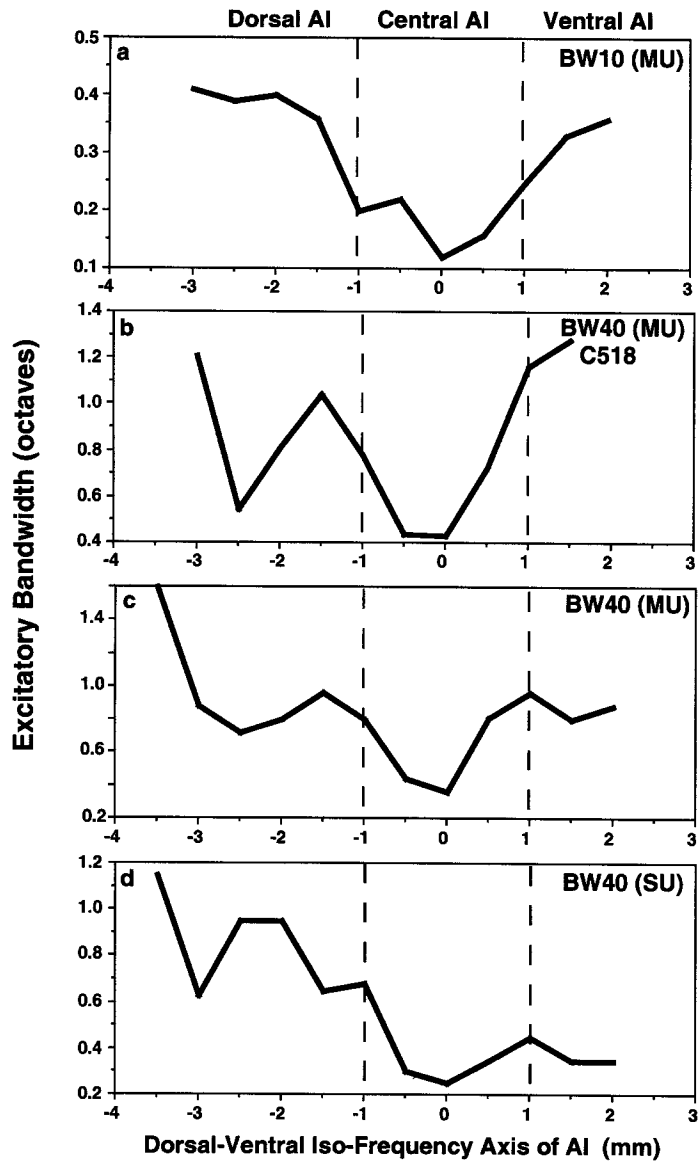


← **Figure 1** Frequency tuning properties of cortical neurons. (a) Examples of pure-tone frequency tuning curves. (*Lighter shading*) Frequency/intensity combinations for pure tones that produce an excitatory response of the neurons. The frequency evoking responses at the lowest intensity is termed characteristic frequency (CF). (*Left*) A narrowly tuned neuron with a maximal frequency extent or bandwidth (*BW*) of less than one half an octave either 10 or 40 dB above threshold (*dashed lines* labeled BW10 and BW40). (*Right*) A broadly tuned neuron. Its excitatory bandwidth is strongly dependent on stimulus intensity with  $BW_{10} = 1$  octave and  $BW_{40} = 3$  octaves. (b) Examples of two-tone tuning curves. Moderate activity is evoked by a fixed tone whose frequency falls within the excitatory tuning curve, approximately 10 dB above response threshold (*black dot*). A simultaneously presented second tone of various intensity and frequency combinations can enhance the activity (*light shades*, excitatory regions) or reduce the response to the fixed tone (*dark shades*, inhibitory regions). (*Left*) A narrow excitatory tuning curve and two broader inhibitory sidebands, one on each side the CF. (*Right*) A narrow excitatory tuning curve that exhibits three inhibitory sidebands. Two narrow, low-threshold inhibitory sidebands are discernible on the low-frequency side of the CF. A single, high-threshold inhibitory sideband can be seen on the high-frequency side. (c) Distribution of sharpness of tuning 10 and 40 dB above minimum threshold. The sharpness of tuning is expressed as *Q* factor, i.e. the CF is divided by the linear bandwidth. The relative distribution for 803 single and multiple units from cat primary auditory cortex (AI) is shown (CE Schreiner, unpublished observation). The mean  $Q_{10}$  was  $4.43 \pm 2.97$  and the mean  $Q_{40}$  was  $1.67 \pm 1.21$ .

tenth of an octave or wider than five octaves. As demonstrated by the distribution of  $Q_{10}$  and  $Q_{40}$  values shown in Figure 1c, on average the bandwidth increases systematically with stimulus intensity.

The spatial distribution of the excitatory bandwidth along the iso-frequency domain or dorso-ventral axis of the ectosylvian gyrus of cat AI is nonuniform and can be divided into three distinct subregions. Figure 2a shows the spatial distribution of *BW* values 10 dB above response threshold for multiunit responses. The ventral portion of the mapped area, the region bordering the second auditory field (AII), usually shows frequency RFs of wide bandwidths. This broad excitatory bandwidth as measured with multiunit responses indicates wide-range spectral convergence (Schreiner & Cynader 1984, Schreiner & Mendelson 1990, Heil et al 1992, Schreiner & Sutter 1992). The *BW* values decrease gradually toward the center of AI, reaching a minimum about 2–3 mm dorsal of the AI/AII border. This central portion with narrow excitatory frequency tuning and a strict cochleotopic gradient can be most readily equated with the classic primary auditory field (Merzenich et al 1975, Reale & Imig 1980). Dorsal to the central portion of AI,  $BW_{10}$  and the width of the corresponding frequency filter generally increase.

As mentioned, bandwidth values of frequency tuning curves in AI depend strongly on stimulus intensity (see Figure 1a,c). At low stimulus intensities neurons are usually more frequency-selective or exhibit RFs of distinctly narrower bandwidth than at higher intensities. However, a relative intensity independence



← **Figure 2** Spatial distribution of excitatory bandwidth measures in the iso-frequency domain of cat primary auditory cortex (AI). (a) Mean excitatory bandwidth of multiple-unit (MU) responses 10 dB above threshold is plotted as a function of location along the iso-frequency domain (modified from Schreiner & Sutter 1992). The bandwidth, expressed in octaves, was averaged in bins 0.5 mm wide over several animals. Position zero millimeters corresponds to the location with the narrowest tuning in each individual case. (Dashed lines) Approximate extent of the central, narrowly tuned region of AI (central AI). The adjacent, more broadly tuned regions are labeled dorsal AI and ventral AI, respectively. (b) Excitatory bandwidth 40 dB above threshold for one individual case (C518; modified from Schreiner & Mendelson 1990). (c) Mean excitatory bandwidth 40 dB above threshold for multiple-unit responses (modified from Schreiner & Sutter 1992). (d) Mean excitatory bandwidth 40 dB above threshold for single-unit responses (SU) (modified from Schreiner & Sutter 1992). Note the reduction in bandwidth in ventral AI compared with c.

can be found for some narrow-band neurons in the center portion of AI. Moreover, some neurons can show a decrease in bandwidth at higher intensities, even to the degree of nonresponsiveness. This behavior has usually been interpreted in the context of intensity tuning (Erulkar 1956, Greenwood & Maruyama 1965, Brugge et al 1969, Phillips & Irvine 1981, Suga & Manabe 1982, Phillips & Orman 1984, Phillips et al 1985, Phillips & Hall 1987, Schreiner et al 1992, Sutter & Schreiner 1995).

The differences in excitatory bandwidth for low- and high-stimulus intensities is reflected in the spatial distribution of these values along the iso-frequency axis. The spatial distribution of *BW10* forms a gradient of narrow-to-broad from central to dorsal AI. *BW10*s in central AI are also significantly more narrow than in ventral AI. These distinctions have been, in fact, the basis for the division of AI into three subregions. When bandwidths at 20–40 dB above response threshold are mapped across the surface of AI, a more complex pattern of spatial segregation emerges for broad and narrow bandwidths (Figure 2*b,c*). In the central and ventral region of AI, the spatial distribution of bandwidth at increasingly higher stimulus intensities is usually similar to that of *BW10* (Figure 2*b,c*). However, a second cluster of neurons with narrow-band frequency tuning can be observed for higher-stimulus intensities approximately 2 mm dorsal to the central band of narrow tuning. The narrow-band clusters are interleaved with similarly clustered broadband neurons (see Figure 2*b,c*). This interleaved or modular pattern of intensity-dependent integration properties on the iso-frequency axis is clearly reflected in the point-spread distribution evoked by a single pure tone at different intensity (Phillips et al 1994, Schreiner 1998). These data suggest that AI contains several subregions when assessed with intensity-sensitive spectral integration measures.

This distinct and consistent topographical pattern of integrative bandwidth suggests the view of a modular functional organization of AI. In addition, it provides a framework for the investigation of other functional organization principles in the iso-frequency domain. This is useful because, usually, positions within the iso-frequency domain are difficult to define and compare from animal

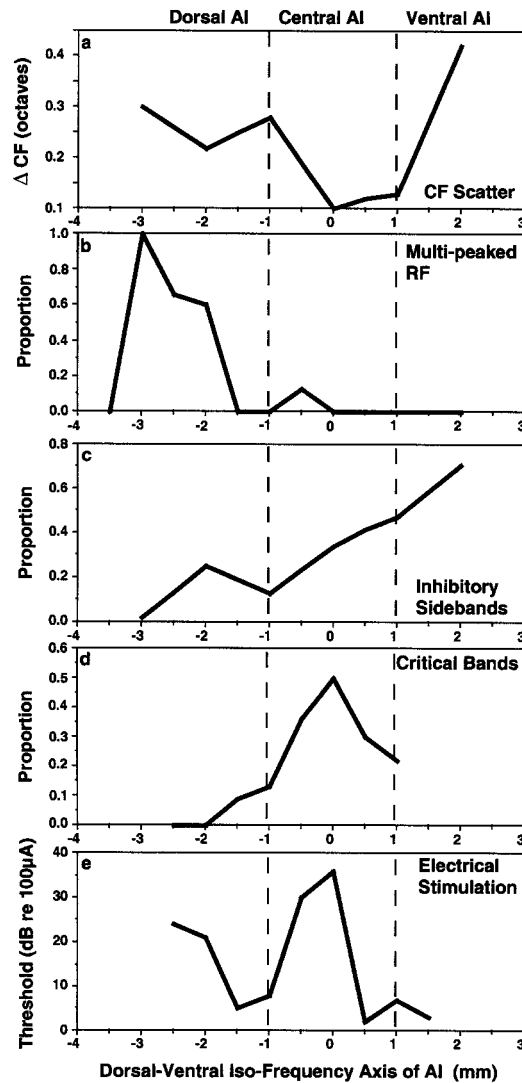
to animal. Anatomical landmarks, such as the location of sulci, and functional landmarks, such as different binaural bands, are generally highly variable and difficult to align (Kawamura 1971, Merzenich et al 1975). By contrast, the topography of the excitatory bandwidth provides a convenient spatial reference that is simple in structure, relatively easy to ascertain, and reliable at least for cats and monkeys.

Some interesting similarities and differences between single and multiunit responses are observed in the topographic distribution of excitatory bandwidth on the iso-frequency axis. Although the topographical gradients of *BW40* are similar for multiple and single unit responses in central and dorsal AI, there is no clear bandwidth gradient for single units in ventral AI (see Figure 2*d*). Most individual ventral neurons are narrow-band for frequency, whereas multiple-unit responses were progressively more broad-band toward the border of AII (Schreiner & Sutter 1992). The discrepancy between single and multiunit recordings in ventral AI suggests that the scatter in CF of nearby cells progressively increases toward the ventral border of AI. An experimental assessment of the local CF scatter supports that hypothesis (Schreiner & Sutter 1992). A distinct minimum in the local CF scatter is found in the central region of AI with increasing CF scatter toward the dorsal and, in particular, the ventral border of AI (Figure 3*a*). This pattern of local CF scatter also supports a functional division of AI into three distinct parts and provides evidence for a systematic variation in the convergence of frequency information into the iso-frequency domain of AI, with direct implications for local spectral integration characteristics.

***Multipeaked Tuning Curves*** Most frequency tuning curves in AI are single peaked (Phillips & Irvine 1981), i.e. they have a single region of low-intensity responses centered at the CF. However, tuning curves with two or three distinct low-threshold peaks, so-called multipeaked tuning curves, have also been described (Oonishi & Katsuki 1965, Abeles & Goldstein 1972, Sutter & Schreiner 1991, Dear et al 1993, Wenstrup & Grose 1995, Fitzpatrick et al 1998b). Relating the position of single neurons with multipeaked tuning curves to the excitatory bandwidth distribution in AI reveals a distinct spatial distribution of these neurons (Sutter & Schreiner 1991). Multipeaked tuning curves are primarily found 2–3 mm dorsal to the narrow-band center of AI, whereas the central and ventral regions of AI show little evidence of single neurons with multiple frequency response areas (see Figure 3*b*). This subpopulation of cortical neurons may be sensitive to specific spectro-temporal combinations in the acoustic input (Sutter & Schreiner 1991, He et al 1997). The spatial clustering of these specialized multipeaked neurons implies a functional segregation. Thus spatial and functional segregation appears to be a general organizing principle of AI.

The region of functional transition between central AI and dorsal AI parametrically defined in this review is well within the more strictly defined core area of AI; it is not a reflection of the beginning of either the “dorsal zone” or the “sylvian fringe.” These latter regions are vaguely defined regions that have been

**Figure 3** Spatial distribution of measures related to spectral integration in the iso-frequency domain of cat primary auditory cortex (AI). Position zero millimeters corresponds to the location with the narrowest tuning in each individual case. (a) Mean local scatter of characteristic frequency (CF) is plotted as a function of location along the iso-frequency domain (modified from Schreiner & Sutter 1992). Local CF scatter is defined as the amount of frequency difference ( $\Delta$  CF) between the CF of an individual neuron and the tonotopic map based on all other neurons in a map of AI. (b) Distribution of neurons with multi-peaked frequency tuning curves or receptive fields (RFs) in AI (modified from Sutter & Schreiner 1991). (c) Distribution of neurons with two inhibitory sidebands in AI (Sutter et al 1999). These neurons had a single inhibitory band on each side of the excitatory region. (d) Distribution of neurons with level-tolerant bandwidth as well as a bandwidth equal to or narrower than the behaviorally determined critical bandwidth (modified from Ehret & Schreiner 1997). The physiological bandwidth was determined using a paradigm of noise-on-tone masking (see text). (e) Minimum response threshold of cortical sites to cochlear electrical stimulation (modified from Raggio & Schreiner 1999). Electrical stimulation consisted of single bipolar pulses of 200  $\mu$ s/phase using a bipolar cochlear electrode pair.



shown to differ from the core area of AI in their functional properties and their thalamocortical connectivity (Middlebrooks & Zook 1983, Brandner & Redies 1990, He & Hashikawa 1998). However, delineating a precise border between dorsal AI proper and the adjacent auditory field, the dorsal zone (see Figure 5), is difficult because the response properties of neurons in this region are not homo-

geneous (He et al 1997, Sutter & Schreiner 1991). This question has also been raised in AI of mustached bats (Fitzpatrick et al 1998a,b). Accordingly, unambiguous criteria for the definition of such a boundary have not emerged yet, and the issue of the exact location of the dorsal border of AI remains unresolved.

In summary, at least three functionally distinct regions along the iso-frequency domain of cat AI can be identified with pure-tone stimulation. They are distinguished by the shape and bandwidth of excitatory frequency tuning curves and the scatter of CF in spatially adjacent neurons. Central AI is dominated by narrow-band neurons. Ventral AI also has many narrow-band neurons, however, with a larger CF scatter. Dorsal AI can be distinguished from central and ventral AI by a fairly high percentage of broad tuning curves and tuning curves with multiple, distinct excitatory response regions, implying specific integrative rules. In addition, dorsal AI contains a second circumscribed region with narrow-band neurons. These spatial distributions of the bandwidths of cortical frequency RFs are closely related to spectral integration properties and demonstrate a systematic functional organization of AI with regard to spectral resolution. Similar results were obtained in AI of owl monkeys, squirrel monkeys, ferrets, and possibly bats (Recanzone et al 1999, Cheung et al 1997, Shamma et al 1993, Fitzpatrick et al 1998a) and likely represent a general processing principle of AI. Auditory cortical fields other than AI may contain similar organizations. Evidence for a bandwidth or spectral integration gradient has been obtained in a nonprimary field in monkeys (Rauschecker et al 1995). Other fields, such as the posterior auditory field (Phillips & Orman 1984, Heil & Irvine 1998) or the anterior auditory field in cats (Eggermont 1998; CE Schreiner, unpublished observations) show ranges of bandwidth for pure-tone RFs similar to those seen in AI, but no clear spatial organization with respect to spectral integration has yet been revealed in these nonprimary fields.

The systematic change in spectral selectivity across AI is significant for understanding the cortical representation and processing of spectrally complex signals, like species-specific vocalizations, speech, music, and ambient noise. These topographies suggest that any incoming signal is simultaneously processed through many filters with different center frequencies and a broad range of bandwidths. Spectral information in AI is extracted and represented by multiple modules for frequency resolution along the iso-frequency domain, and the center frequency of each bandwidth module is aligned to the “frequency decomposition” or tonotopic axis (see Figure 5). Signal analysis by neurons with a range of RF sizes has also been proposed for the visual system (Graham 1989). Parallel analysis by multiple bandwidths results in a topographically distinct representation of information within the iso-frequency domain differentially weighted by filter width. Such a parallel “multiresolution analyzer,” which is similar to a wavelet analysis design, may prove ideal for the extraction and evaluation of complex spectral shapes, e.g. formant structure of vowels and integrated acoustic properties of phonetic features (Jakobsen et al 1963, Blumstein & Stevens 1979, Shamma et al 1993, Schreiner & Calhoun 1994, Wang & Shamma 1995).

## Inhibitory Surrounds of Excitatory Tuning Curves Shape Spectral Integration

Variations in the distribution of GABAergic neurons between cortical layers as well as in the horizontal extent of layers in AI (Prieto et al 1994) strongly suggest that local cortical processes contribute to the distribution of inhibitory properties and the topography of spectral integration. The spectral properties of inhibition should play an important role in shaping a neuron's response to complex behaviorally relevant stimuli (e.g. Suga & Tsuzuki 1985, Ehret 1995, Suga 1995). Therefore, one would expect to find functional organization with respect to inhibitory RF properties in AI.

The majority of central auditory neurons have distinct inhibitory "sidebands," i.e. circumscribed inhibitory regions in the frequency RF that extend beyond the borders of the excitatory region. The frequency RF properties of this inhibition are instrumental in shaping the spectral integration profile of auditory neurons (Ehret 1995, Ehret & Schreiner 1997, Calhoun & Schreiner 1998, Shamma et al 1995, Wang et al 1996, Taha et al 1996). Inhibitory influences are particularly evident in responses to broad-band or spectrally complex sounds that have energy extending into the inhibitory regions. They are less evident in low-intensity pure-tone stimulation with frequency content that does not overlap with inhibitory regions. To establish relationships between excitatory bandwidth and inhibitory surrounds, and the possibility of a topographical mapping of inhibitory RFs across AI, a recent study systematically explored shape and position of the inhibitory RF components by using a two-tone paradigm (Sutter et al 1999).

In the two-tone paradigm, a soft excitatory tone at CF is paired with a second tone of variable frequency and intensity. Inhibitory regions in the frequency/intensity plane of the second tone are characterized by a response to both tones that is statistically below the response to the CF tone alone. Figure 1*b* shows two examples of two-tone tuning curves that contain a simple and a more complex arrangement of inhibitory frequency RFs.

The two-tone paradigm is useful for three reasons. First, inhibitory sidebands can be observed in cells with very low spontaneous activity, as is often the case in AI. Second, two-tone nonlinear response profiles are highly predictive of a cell's response to more complex sounds (Nelken et al 1994a-c, Shamma & Versnel 1995). Finally, in the visual system, nonlinear spatial integration has been shown to play a role in perceptual processes, such as figure/ground segmentation; however, such integration effects cannot be observed with single bars or spots of light (Knierim & van Essen 1992, Kapadia et al 1994, Zipser et al 1996).

In general, neurons in cat AI are characterized by heterogeneity in the properties of their inhibitory frequency tuning curves (Sutter et al 1999). Approximately one third of cells exhibits a simple inhibitory surround structure with one narrow inhibitory band for frequencies above CF and one, usually broader, inhibitory band for frequencies below CF. A similar profile is commonly seen in the subcortical auditory system. Other neurons have more complex inhibitory sur-

rounds with either very broad inhibitory frequency ranges or multiple inhibitory regions on either side of the excitatory response area (Figure 1*b*). Cells with three to five distinct inhibitory regions comprise approximately 40% of AI neurons. This suggests that a high percentage of AI neurons have complex inhibitory spectral RFs that can extend far beyond the frequencies included in the classical single-tone tuning curve. The topographical distribution of inhibitory RFs indicates a nonuniform distribution along the iso-frequency domain. Cells with complex inhibitory surrounds are significantly more common in dorsal AI. Conversely, the majority of cells in central and ventral AI have only one upper and one lower inhibitory band (Figure 3*c*). The variety of inhibitory band structures indicates that AI neurons can be involved in more complex spectral analysis than simple band-pass filtering. Based on the complexity of the excitatory and inhibitory RF structure of neurons in dorsal AI, these cells appear to be well suited to analyzing highly structured sound spectra, for example those related to resonances in the vocal tract in communication sounds and in the pinna of the outer ear for sound localization information. Cells in central and ventral AI appear to view the world through a simpler frequency band-pass “aperture.” Thus, the distribution of inhibitory response properties reflects and, possibly, shapes the modular organization of spectral integration/resolution properties.

### Spectral Integration Estimated with Ripple Spectra is Related to Frequency Tuning Curves

The coding of signals with broad-band spectra or spectral shapes that are common in speech and animal communication has been suggested as an important functional goal of the AI (Schreiner & Calhoun 1994, Shamma et al 1993, Wang & Shamma 1995). The need for studies of complex spectra is emphasized by the difficulty in predicting the response to spectrally complex signals from pure-tone frequency RFs (e.g. Creutzfeldt et al 1980, Schreiner & Langner 1988b, Nelken et al 1994a–c). Recently, several studies used spectrally complex but parametrically accessible signals to explore the responses of cortical neurons to broad-band stimuli (e.g. Schreiner & Calhoun 1994, Shamma et al 1995, deCharms et al 1998, Escabi et al 1998). One approach is to use sounds with “ripple” spectra that have a broad-band carrier signal with a sinusoidal modulation of its spectral envelope, i.e. systematic intensity variations along the frequency axis of the spectrum (Schreiner & Calhoun 1994, Calhoun & Schreiner 1998, Shamma et al 1995, Shamma & Versnel 1995, Kowalski et al 1996). These ripple spectra are directly analogous to spatial gratings used in the exploration of the visual system (e.g. Campbell et al 1970), with frequency in the ripple spectra directly analogous to azimuth in a vertical sine wave grating. By changing (*a*) the spectral modulation frequency (analogous to spatial frequency in visual gratings), (*b*) the modulation depth of the spectral envelope (analogous to contrast in visual gratings), and (*c*) the phase of the spectral modulation frequency, a systematic evaluation of responses to a certain class of spectrally complex signals can be achieved. A

similar approach in the visual system has provided evidence that signal properties outside the classical spatial RF can significantly influence and contribute to the response behavior (e.g. DeValois & DeValois 1988). Accordingly, auditory cortical responses may reflect cumulative effects of excitatory and inhibitory influences and effects from regions outside the classical RF that are usually not seen with pure tones. Another advantage of ripple stimuli is that this class of sounds is closely related to the resonance structure of the vocal tract and, therefore, to spectra of natural vocalizations (Shamma & Versnel 1995).

Comparison of the excitatory and inhibitory regions of the RF found with the two-tone paradigm are in reasonable agreement with the responses obtained with ripple spectra (Shamma et al 1995, Calhoun & Schreiner 1998). Correlation analysis between responses to ripple spectra and two tones show a weak but consistent relationship between the two RF measures. In particular, the ripple density that produces the strongest response (analogous to the preferred spatial frequency in the visual system) is more strongly correlated with the spectral spacing between excitatory and inhibitory subregions than with the width of the excitatory bandwidth alone (Calhoun & Schreiner 1998). These findings support the notion that responses to broad-band stimuli are shaped by an interaction of inhibitory and excitatory RFs. In addition, response properties derived with ripple spectra appear to be nonuniformly distributed across AI (Versnel et al 1995).

### Neuronal Critical Bands Estimated by Masking of Tone Responses Correlate with Excitatory Bandwidth

Although the spectral RFs of auditory cortical neurons derived from tones or ripple spectra are useful for estimating properties of spectral integration, a more direct measure of the auditory filter or critical bandwidth is necessary to establish a close relationship between psychophysics and neuronal behavior. To this end, a recent study (Ehret & Schreiner 1997) used a masking paradigm that is analogous to psychophysical measurements of critical bands to determine the critical bandwidth of single neurons in AI. The task was accomplished by assessing the minimum necessary bandwidth of a band-pass noise masking sound to suppress the response to a simultaneously presented tone (see Ehret & Merzenich 1985, 1988; Ehret & Schreiner 1997). By repeating this measurement with different tone intensities, the intensity dependence of the neural critical bandwidth can be assessed. The frequency dependence of the critical band can be obtained by repeating this measurement for neurons with different CFs.

The study revealed that about two thirds of the sampled neurons in AI show spectral integration properties that remain relatively constant with varying intensity (i.e. they were intensity tolerant). However, the critical bandwidth of many intensity-tolerant neurons was broader than predicted from behavioral measurements of the critical band. Neurons that were intensity tolerant and had critical bandwidths similar to the behaviorally known values for cats (Pickles 1975, Nien-

huys & Clark 1979) were less common and were concentrated in central AI (Figure 3*d*).

In the same study, the excitatory spectral RF was characterized with pure tones, allowing a direct comparison of pure-tone measures of spectral integration with critical band measures. For some neurons, the spectral integration estimated with pure tones matched closely that for the masking-noise conditions. However, for many neurons there were large discrepancies between the two measures (Ehret & Schreiner 1997). The integration bandwidth determined with the masking noise could be either narrower or broader than the pure-tone tuning curve. Intensity tolerance also could differ significantly between the two estimates. These findings indicate that the actual spectral integration properties depend on the specific stimulus conditions and cannot be inferred from one measure alone. It underscores the point made previously for two-tone and ripple stimuli that pure-tone excitatory measures are not sufficient to explain broad-band behavior, and inhibitory contributions have to be taken into account.

In sum, it appears that a subpopulation of neurons in AI shows spectral integration behavior that closely matches that of psychophysical critical bands. These neurons are concentrated in central AI. However, the spectral integration properties of the majority of neurons, especially in dorsal AI, do not behave as level-tolerant auditory filters of fixed bandwidth and could provide the substrate of noncritical-band spectral integration.

### Indirect Estimation of Spectral Integration with Electrical Cochlear Stimulation Reveals Subregions in Primary Auditory Cortex

Exploration of functional topography in AI of deafened cats with electrical cochlear stimulation provides further evidence for a division of AI into three functionally distinct regions. Electrical stimulation at a fixed location in the cochlea with low-current electrical pulses excites neurons in the spiral ganglion, which, in turn, activates more central auditory stations, including the AI (e.g. Hartmann et al 1997, Dinse et al 1997, Raggio & Schreiner 1999). Comparison with acoustic stimulation shows that the location of excitation in AI corresponds closely to the cochleotopically appropriate stimulation location (Raggio 1992, Dinse et al 1997). However, when obtaining the minimum current levels necessary to evoke a cortical response, three regions of different threshold values can be distinguished along the dorso-ventral iso-frequency extent of cat AI (Raggio 1992, Raggio & Schreiner 1999). Regions of low response thresholds in dorsal and ventral AI are separated by a narrow region of high response thresholds (see Figure 3*e*). This “electrical” high-threshold region appears to run along the entire anterior-posterior tonotopic axis of AI. Comparison to acoustic response properties reveals that the electrical high-threshold region coincides with the central, narrow-band region seen with acoustic stimulation (Raggio 1992).

The high response thresholds in the central region are unexpected because this region usually shows very low response threshold for acoustical stimulation (Schreiner et al 1992). The high thresholds are likely a consequence of strong inhibitory effects in combination with normal spectral integration mechanisms and the broad-band stimulus characteristics due to the spread of electrical stimulation. The reliable feature of functional banding across AI into regions with high and low electrical response thresholds lends further support to the notion that AI is not functionally uniform but shows distinct subregions. The electrical stimulation study shows that such a modular structure is even present after many years of deafness and with limited auditory experience (Raggio & Schreiner 1999), which suggests a fundamental nature of this organization.

## NEUROANATOMY OF SPECTRAL INTEGRATION IN PRIMARY AUDITORY CORTEX

Thalamocortical and intrinsic corticocortical connection patterns of AI also indicate a modular organization of this structure. Single thalamocortical fibers branch and terminate in patches in layers III and IV of rabbit (McMullen & de Venicia 1993) and cat AI (Huang & Winer 1998). Individual neurons in the ventral division of the medial geniculate body can be double labeled when two tracers are injected at different dorsoventral positions along the iso-frequency axis (Read et al 1999). Thus, spatially segregated subsets of neurons along the iso-frequency axis of AI share a common input from the thalamus. It is possible that subregions of AI that receive common thalamic input also mutually innervate each other via horizontal connections in layer III. Although no direct comparisons between thalamocortical and intrinsic modules in AI have been made, the patchy patterns generated by these two subcircuits share a similar spatial order. Thalamocortical patches in rabbits and cats are segregated by approximately 1.5 mm. Adjacent intrinsic clusters of AI neurons in cats are segregated by spatial intervals of the same range (see Figure 4) (Read et al 1998, Wallace et al 1991).

Recently, we described a correlation between anatomic and physiologic modules on the iso-frequency axis (Read et al 1998). Long-range intrinsic cortical connections in AI occur between clusters of neurons with similar CFs in an elongated patchy pattern that follows the physiologic dorsoventral iso-frequency axis. The mean CF value of dorsal retrograde labeled neurons is within one third of an octave. Thus, dorsal anatomic patches project to central neurons with similar CFs. That is, intrinsic anatomic connections with the central region are indeed confined to the iso-frequency axis (Clarke et al 1993; Rouiller et al 1991; Read et al 1998, 1999).

The pattern of intrinsic connectivity along the iso-frequency axis is discontinuous or patchy, indicating that a submodality other than CF determines this pattern. It has been suggested that binaural interaction properties are not the source

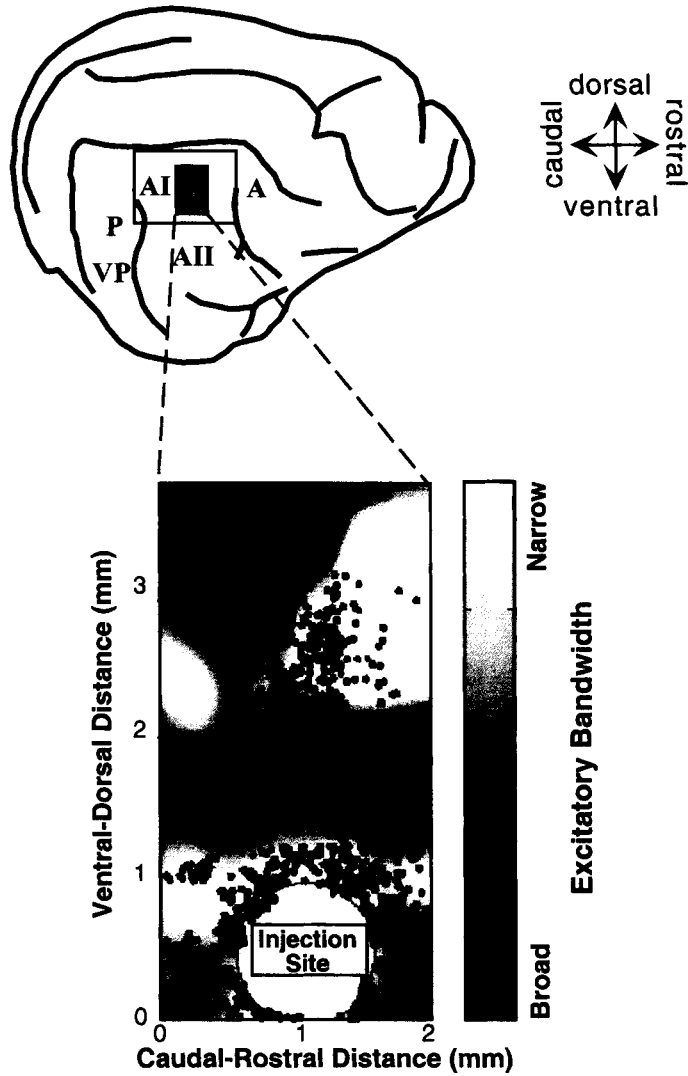


**Figure 4** Example of patchy intrinsic connectivity in cat primary auditory cortex (AI) that is closely related to distribution of excitatory bandwidth (modified from Read et al 1998). (*Rectangular region*) Represents a portion of AI in the high-frequency region (8–14 kHz). (*Background shading*) Corresponds to the sharpness of tuning 40 dB above threshold. (*Contour lines*) Separate narrow-band (*light shading*) from broad-band (*dark shading*) regions. A retrograde tracer was injected into the narrow-band region in central AI (*circle*). (*Dots*) Labeled neurons that project to the injection site. A large dorsal cluster of labeled neurons coincides with a second narrow-band region in dorsal AI.

of the pattern (Matsubara & Phillips 1988). Injections of retrograde label into the central narrow-band region reveals a prominent dorsal anatomic patch that coincides with the dorsal cluster of neurons with narrow *BW*<sub>40</sub> (Figure 4). That is, narrow-band neurons in dorsal AI project to the narrow-band neurons in central AI. A fundamentally different and more complex anatomic pattern, including a large degree of frequency convergence from patches outside the iso-frequency axis, was observed with injections into the broad-band subregions of dorsal and ventral AI (Read et al 1998, 1999; Kadia et al 1999). Thus, neuroanatomical connectivity studies reveal two different modes of cortico-cortical frequency convergence in AI that are likely to give rise to different modes of spectral integration: The narrow-band mode is limited to like frequencies, whereas the broad-band mode utilizes cortical convergence over a wide range of frequencies. The connectivity of the broad-band system is reminiscent of the patchy organization in visual cortex that joins similar response properties across different locations on the receptor surface (Boskin et al 1998). In contrast, the narrow-band system appears to represent another principle because it connects regions with similar bandwidth properties in the iso-frequency domain.

Combined, these data provide anatomical evidence for at least two spatially segregated systems of spectral integration in the AI that may be related to the distinction between critical-band and noncritical-band integration behavior. The anatomic and physiologic segregation of two distinct, interleaved spectral integration modules within AI may reflect a bottom-up segregation compatible with a spectro-temporal multiscale representation (Schreiner & Calhoun 1994, Shamma et al 1995, Wang & Shamma 1995), which has evolved to accommodate inherent trade-offs in efficiency when extracting multiple features from natural sounds. Such processing may be similar to principles of spatial multiscale resolution in the visual system (e.g. Marr 1982, Graham 1989). The proposed functional segregation of AI into dorsal, central, and ventral subregions was initially conceived to distinguish the central narrow-band region from the adjacent, generally more broad-band regions of AI. Further analysis uncovered other functional aspects that differed between the three regions and confirmed the appropriateness of delineating functional clusters. The neuroanatomical findings of different and specific intracortical connectivities for the subregions provides further evidence for modularity in the iso-frequency or spectral integration domain of AI.

## REPRESENTATION OF MULTIPLE ACOUSTIC PARAMETERS IN PRIMARY AUDITORY CORTEX

Functional and structural patchiness has been used to argue against the existence of consistent parameter gradients in the organization of the iso-frequency domain. However, from considerations of self-organizing models (e.g. Kohonen 1984, Kohonen & Harii 1999, Obermayer et al 1990) it appears that topographical

gradients and local patches are both necessary consequences of self-organizing algorithms optimized for analyzing stimuli with many parameters and preserving topology. Although we have focused here on two simple information-bearing parameters, the center frequency and the bandwidth of auditory filters, many other relevant parameters are also mapped onto the surface of AI. These include, but are not limited to, response latency (Mendelson et al 1997, Wang et al 1995), preferred sound intensity (Heil et al 1994, Schreiner et al 1992, Phillips 1990), amplitude modulation properties (Eggermont 1998), frequency modulation rate and direction (Mendelson et al 1993), and binaural interaction characteristics (e.g. Clarey et al 1992, 1994; Brugge & Imig 1978; Kelly & Judge 1994; Middlebrooks et al 1980; Imig & Adrian 1977; DC Fitzpatrick & S Kuwada, personal communication). The full range of behaviorally useful parameters can be expected to be represented across AI, perhaps with overrepresentation of behaviorally important parameter ranges (Suga 1977, 1984). To provide a wide range of combinations between the different information-bearing parameters, complex spatial relationships between the various parameter maps, similar to those seen between different RF properties in primary visual cortex, are necessary.

From this point of view, each neuron and each location in AI can be understood as representing a specific set of many independent variables (stimulus dimensions). Topographically, each location on the cortical surface corresponds to a specific intersection of systematic “maps” of each parameter. Mathematically, this can be described as a response vector with specific direction and length in a multidimensional parameter space (e.g. Lennie 1998). Although many different parameters are mapped on the cortical surface, we can gain insight into cortical processing by plotting two variables at a time, such as frequency versus time. However, even these “spectro-temporal RFs” (Eggermont et al 1983, deCharms et al 1998) represent only a fraction of the actual underlying parameters that contribute to the response of a neuron (Escabi & Schreiner 1999).

It is conceivable that the subregions of AI represent information-bearing parameters that are specifically suited for different tasks. Central AI, with its narrow tuning and high incidence of neurons with critical-band behavior, may be particularly suited for signal detection and other tasks ascribed to narrow-band analysis, such as masking and loudness summation (e.g. Moore 1997, Scharf 1970, Zwicker et al 1957). The more broadly tuned and spectrally complex integration region in dorsal AI may be more suitable for noncritical-band integration for the analysis of cross-frequency properties such as spectral shape and temporal synchrony (Nelken et al 1999, Sutter & Schreiner 1991). Ventral AI, with fairly narrowly tuned neurons but a high degree of CF scatter and frequency convergence, may be well suited for short-range interactions between neurons with a wide range of CFs. By means of cortical representational plasticity, these relationships may be formed by and adjusted to behavioral challenges throughout life (Buonomano & Merzenich 1998). The observed functional and anatomical modularity in AI appears to be fundamentally related to general cortical processing principles. The interpretation of the role of modularity within a given field and

its relationship to modular or distributed models of sensory processing and perception across many auditory stations hinges on interpretations of the neuronal code (see deCharms & Zador 2000) and requires further studies in conjunction with behavioral and psychophysical tasks.

## SUMMARY AND CONCLUSIONS

It is clear that at the level of AI there are no uniform properties of auditory filters. The range of spectral integration in AI was found to vary widely no matter how spectral integration was probed: with single tones, two tones, ripple noise, masking of tones by broad-band noise, or electrical stimulation. Instead, there are for any given center frequency a range of filter bandwidths, reminiscent of a multi-resolution or multiple bandwidth analysis. AI neurons also exhibit a variety of level tolerances. The range of filter properties includes neurons with bandwidths and level tolerance compatible with properties of psychophysical critical bands. Such neurons are most common in a fairly small region, namely central AI. By contrast, many neurons in AI exhibit spectral integration properties that are reminiscent of psychophysical processes that involve noncritical-band behavior. They are predominantly found in dorsal AI and may be particularly suited to perform integration across a wider frequency range. In other words, single-unit properties and spatial organization of AI can provide a basis for the explanation of various psychophysical phenomena related to spectral integration (e.g. Nelken et al 1999). However, the actual role that these neurons play in the creation of perceptual attributes remains to be tested. Based on the wide variety of spectral integration properties and their spatial distribution along the iso-frequency axis, it can be concluded that the layout of AI accommodates two fundamental processing strategies: One axis of cortical organization, the frequency domain, reflects the basic frequency decomposition of complex sounds; and the orthogonal axis, the iso-frequency domain, reflects frequency resolution and integration aspects (see Figure 5).

The patchy pattern of intracortical horizontal connections is consistent with a modular, topographical organization of the frequency resolution axis. This modular organization is reflected in the nonuniform distribution of several RF properties and led to the functional subdivision into dorsal, central, and ventral AI. Although these subregions are useful in exploring and describing properties of AI, no precise criteria have been developed for an unambiguous identification of the boundaries between the subregions. They should, therefore, be considered more as heuristic markers than as firm functional or anatomical demarcations.

The consequences of a modular organization for the cortical representation of complex signals in animals may provide a general basis for principles that govern the perception and categorization of speech and music in humans. There are at least two interpretations of the observed form of functional organization. One view would hold that the global organization of AI can be understood as the

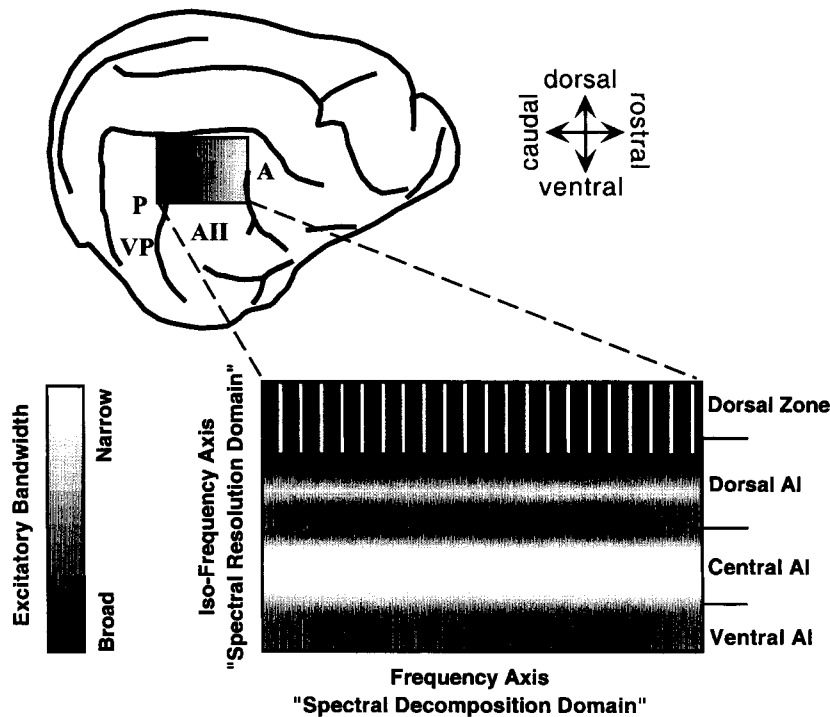


**Figure 5** Functional organization of spectral analysis in cat primary auditory cortex (AI). According to this schematic depiction, AI consists of a spectral decomposition organization in the rostro-caudal axis (see shading in small inset) and a spectral resolution organization in the dorsal-ventral axis (see shading in enlarged region). The spectral resolution domain along the iso-frequency axis shows systematic variations in the bandwidth over which spectral integration is performed. Based on these variations, AI can be divided into three subregions. Dorsal AI may partially overlap with the dorsal zone (*white hatching*, or *white vertical lines* at top of enlarged region), a functionally distinct region at the most dorsal extent of the ectosylvian gyrus.

overlaid topographical representation of several independent information-bearing parameters of sound that are sufficient to decompose and characterize complex sounds and auditory scenes (e.g. Suga 1977, 1984; Schreiner 1995, 1998). In this scenario, modularity reflects multiple representations of the value ranges of parameters that are necessary for allowing sufficient combinations between many functional parameters. Well-known examples of this principle are the presence of repeated binaural interactions bands in AI (Imig & Adrian 1977, Middlebrooks et al 1980, Brugge & Imig 1978) or ocular dominance bands in V1 (Hubel & Wiesel 1962). Another view, which is not mutually exclusive, would be to regard

functionally distinct regions or modules in AI as functional “foveas” for specific tasks. An example would be the expanded region of the echolocation frequencies in bat AI (Suga 1977, 1984). Both interpretations suggest a capacity of AI to perform in parallel analyses of frequency content, sound intensity, and sound source location. They are also compatible with the presence of independent processing streams for different aspects of auditory scene analysis (Bregman 1990), such as stimulus shape and stimulus location (Rauschecker 1998). Evidence for such processing streams is important because it would reveal basic constituent properties of sensory encoding and would allow a more direct experimental approach to each identified component, including analysis of specific perceptual capacities. Understanding the organizational principles of AI and, in particular, its different subregions provides an important step toward determining the relationship between auditory physiology and perception.

#### ACKNOWLEDGMENTS

Work was supported by grants from the National Institute of Deafness and Communicative Disorders (to CES and MLS) and by the Office of Naval Research (to CES).

**Visit the Annual Reviews home page at [www.AnnualReviews.org](http://www.AnnualReviews.org).**

#### LITERATURE CITED

- Abeles M, Goldstein MH. 1972. Responses of single units in the primary auditory cortex of the cat to tones and tone pairs. *Brain Res.* 42:337–52
- Aitkin LM. 1973. Medial geniculate body of the cat: responses to tonal stimuli of neurons in medial division. *J. Neurophysiol.* 36:275–83
- Aitkin LM, Prain SM. 1974. Medial geniculate body: unit responses in the awake cat. *J. Neurophysiol.* 37:512–21
- Aitkin LM, Webster WR. 1972. Medial geniculate body of the cat: organization and responses to tonal stimuli of neurons in ventral division. *J. Neurophysiol.* 35:365–80
- Blumstein S, Stevens KN. 1979. Acoustic invariance in speech production: evidence from measurements of the spectral characteristics of stop consonants. *J. Acoust. Soc. Am.* 63:1478–83
- Boskin WH, Zhang Y, Scholfield B, Fitzpatrick D. 1998. Orientation selectivity and the arrangement of horizontal connections in the tree shrew striate cortex. *J. Neurosci.* 17:2112–27
- Brandner S, Redies H. 1990. The projection from medial geniculate to field AI in cat: organization in the isofrequency dimension. *J. Neurosci.* 10:50–61
- Bregman AS. 1990. *Auditory Scene Analysis: The Perceptual Organization of Sound*. Cambridge, MA: MIT Press
- Brugge JF, Dubrovsky NA, Aitkin LM, Anderson DJ. 1969. Sensitivity of single neurons in auditory cortex of cat to binaural tonal stimulation; effects of varying interaural time and intensity. *J. Neurophysiol.* 32:1005–24
- Buonomano D, Merzenich MM. 1998. Cortical plasticity. *Annu. Rev. Neurosci.* 21:149–86
- Calford MB, Webster WR. 1981. Auditory rep-

- resentation within principal division of cat medial geniculate body: an electrophysiology study. *J. Neurophysiol.* 45:1013–28
- Calford MB, Webster WR, Semple MM. 1983. Measurement of frequency selectivity of single neurons in the central auditory pathway. *Hear. Res.* 11:395–401
- Calhoun B, Schreiner CE. 1998. Spectral envelope coding in cat primary auditory cortex: linear and non-linear effects of stimulus characteristics. *Eur. J. Neurosci.* 10:926–40
- Campbell FW, Nachmias J, Jukes J. 1970. Spatial-frequency discrimination in human vision. *J. Opt. Soc. Am.* 60:555–59
- Cheung SW, Bedenbaugh P, Schreiner CE, Merzenich MM. 1997. Multiple tonotopically organized areas in the squirrel monkey auditory cortex. *Assoc. Res. Otolaryngol. Abstr.* 20:204
- Clarey JC, Barone P, Imig TJ. 1992. Physiology of the thalamus and cortex. See Popper & Fay 1992, pp. 232–334
- Clarey JC, Barone P, Imig TJ. 1994. Functional organization of sound direction and sound pressure level in primary auditory cortex of the cat. *J. Neurophysiol.* 72:2383–405
- Clarke S, de Ribaupierre F, Rouiller EM, de Ribaupierre Y. 1993. Several neuronal and axonal types form long intrinsic connections in the cat primary auditory cortical field (AD). *Anat. Embryol.* 18:117–38
- Creutzfeldt OD, Hellweg FC, Schreiner CE. 1980. Thalamocortical transformation of responses to complex auditory stimuli. *Exp. Brain Res.* 39:87–104
- Dear SP, Fritz J, Haresign T, Ferragamo M, Simmons JA. 1993. Tonotopic and functional organization in the auditory cortex of the big brown bat, *Eptesicus fuscus*. *J. Neurophysiol.* 70:1988–2009
- deCharms C, Blake D, Merzenich MM. 1998. Optimizing sound features for cortical neurons. *Science* 280:1439–43
- deCharms RC, Zador A. 2000. Neural representation and the cortical code. *Annu. Rev. Neurosci.* 23:613–47
- DeValois RL, DeValois KK. 1988. *Spatial Vision*. New York: Oxford Univ. Press
- Dinse H, Godde B, Hilger T, Reuter G, von Seelen R. 1997. Optical imaging of cat auditory cortex cohereotopic selectivity evoked by acute electrical stimulation of a multi-channel cochlear implant. *Eur. J. Neurosci.* 9:113–19
- Eggermont JJ. 1998. Representation of spectral and temporal sound features in three cortical fields of the cat. Similarities outweigh differences. *J. Neurophysiol.* 80:2743–64
- Eggermont JJ, Johannesma PIM, Aertsen AMHJ. 1983. Reverse-correlation methods in auditory research. *Q. Rev. Biophys.* 16:341–414
- Ehret G. 1976. Critical bands and filter characteristics in the ear of the house mouse (*Mus musculus*). *Biol. Cybernet.* 24:35–42
- Ehret G. 1995. Auditory frequency resolution in mammals: from neuronal representation to perception. In *Advances in Hearing Research*, ed. GA Manley, GM Klump, C Koepl, H Fastl, H Oeckinghaus, pp. 387–97. Singapore: World Sci.
- Ehret G. 1997. The auditory cortex. *J. Comp. Physiol. A* 181:547–57
- Ehret G, Merzenich MM. 1985. Auditory mid-brain responses parallel spectral integration phenomena. *Science* 227:1245–47
- Ehret G, Merzenich MM. 1988. Complex sound analysis (frequency resolution, filtering and spectral integration) by single units in the inferior colliculus of the cat. *Brain Res. Rev.* 13:139–63
- Ehret G, Moffat AJM. 1984. Noise masking of tone responses and critical ratios in single units of the mouse cochlear nerve and cochlear nucleus. *Hear. Res.* 14:42–57
- Ehret G, Schreiner CE. 1997. Frequency resolution and spectral integration (critical band analysis) in single units of the cat primary auditory cortex. *J. Comp. Physiol. A* 181:635–51
- Erulker SD. 1956. Single unit activity in the auditory cortex of the cat. *Johns Hopkins Bull.* 39:55–86
- Escabi MA, Schreiner CE. 1999. Non-linear spectro-temporal envelope processing in the cat ICC. *Assoc. Res. Otolaryngol.* 22:218

- Escabi MA, Schreiner CE, Miller LM. 1998. Dynamic time-frequency processing in the cat midbrain, thalamus, and auditory cortex: spectro-temporal receptive fields obtained using dynamic ripple spectra. *Soc. Neurosci. Abstr.* 24:1879
- Evans EF, Pratt SR, Spenner H, Cooper NP. 1992. Comparison of physiological and behavioural properties: auditory frequency selectivity. *Adv. Biosci.* 83:159–64
- Fitzpatrick DC, Olsen JF, Suga N. 1998a. Connections among functional areas in the mustached bat auditory cortex. *J. Comp. Neurol.* 391:366–96
- Fitzpatrick DC, Suga N, Olsen JF. 1998b. Distribution of response types across entire hemispheres of the mustached bat's auditory cortex. *J. Comp. Neurol.* 391:353–65
- Fletcher H. 1940. Auditory patterns. *Rev. Mod. Phys.* 12:47–65
- Graham NVS. 1989. *Visual Pattern Analyzers*. New York: Oxford Univ. Press
- Greenwood DD, Maruyama N. 1965. Excitatory and inhibitory response areas of auditory neurons in the cochlear nucleus. *J. Neurophysiol.* 28:863–92
- Hall JW, Haggard MP, Fernandes MA. 1984. Detection in noise by spectro-temporal pattern analysis. *J. Acoust. Soc. Am.* 76:50–56
- Hartmann R, Shepherd RK, Heid S, Klinke R. 1997. Response of the primary auditory cortex to electrical stimulation of the auditory nerve in the congenitally deaf white cat. *Hear. Res.* 112:115–33
- He J, Hashikawa T. 1998. Connections of the dorsal zone of cat auditory cortex. *J. Comp. Neurol.* 400:334–48
- He J, Hashikawa T, Ojima H, Kinouchi Y. 1997. Temporal integration and duration tuning in the dorsal zone of cat auditory cortex. *J. Neurosci.* 17:2615–25
- Heil P, Irvine DRF. 1998. The posterior auditory P of cat auditory cortex: coding of envelope transients. *Cereb. Cortex* 8:125–41
- Heil P, Rajan R, Irvine DRF. 1992. Sensitivity of neurons in cat primary auditory cortex to tones and frequency-modulated stimuli. II: Organization of response properties along the 'isofrequency' dimension. *Hear. Res.* 63:135–56
- Heil P, Rajan R, Irvine DRF. 1994. Topographic representation of tone intensity along the isofrequency axis of cat primary auditory cortex. *Hear. Res.* 76:188–202
- Helmholtz HLF. 1963. *Die Lehre von den Tonempfindungen als physiologische Grundlage fuer die Theorie der Musik*. Braunschweig, Ger.: Vieweg
- Huang CL, Winer JA. 1998. Laminar patterns of auditory thalamocortical input in the cat: a quantitative approach. *Soc. Neurosci. Abstr.* 24:1881
- Hubel DH, Wiesel TN. 1962. Receptive fields, binocular interaction and functional architecture in the cat's visual cortex. *J. Physiol.* 160:106–54
- Imig TJ, Adrian HO. 1977. Binaural columns in the primary field (AI) of auditory cortex. *Brain Res.* 138:241–57
- Imig TJ, Brugge JF. 1978. Relationship between binaural interaction columns and commissural connections of the primary auditory field (AI) in the cat. *J. Comp. Neurol.* 182:637–60
- Jakobsen R, Fant GM, Halle M. 1963. *Preliminaries to Speech Analysis*. Cambridge, MA: MIT Press
- Javel E. 1994. Shapes of cat auditory nerve fiber tuning curves. *Hear. Res.* 81:167–88
- Kadia SC, Liang L, Wang X, Doucet JR, Ryugo DK. 1999. Horizontal connections within the primary auditory cortex of cat. *Assoc. Res. Otolaryngol. Abstr.* 22:34
- Kapadia MK, Gilbert CD, Westheimer G. 1994. A quantitative measure for short-term cortical plasticity in human vision. *J. Neurosci.* 14:451–57
- Katsuki Y, Wantanabe T. 1959. Activity of auditory neurons in upper levels of brain of cat. *J. Neurophysiol.* 22:343–59
- Kawamura K. 1971. Variations of the cerebral sulci in the cat. *Acta Anat.* 80:204–21
- Kelly JB, Judge PW. 1994. Binaural organization of primary auditory cortex in the ferret (*Mustela putorius*). *J. Neurophys.* 71:904–13
- Kiang NY, Moxon EC. 1974. Tails of tuning

- curves of auditory-nerve fibers. *J. Acoust. Soc. Am.* 55:620–30
- Kiang NY, Sachs MB, Peake WT. 1967. Shapes of tuning curves for single auditory-nerve fibers. *J. Acoust. Soc. Am.* 42:1341–42
- Knierim JJ, van Essen DC. 1992. Neuronal responses to static texture patterns in area V1 of the alert macaque monkey. *J. Neurophysiol.* 67:961–80
- Kohonen T. 1984. *Self-Organization and Associative Memory*. Berlin: Springer
- Kohonen T, Hari R. 1999. Where the abstract feature maps of the brain might come from. *Trends Neurosci.* 22:135–39
- Kowalski N, Depireux DA, Shamma SA. 1996. Analysis of dynamic spectra in ferret primary auditory cortex. I. Characteristics of single-unit responses to moving ripple spectra. *J. Neurophysiol.* 76:3503–23
- Lennie P. 1998. Single units and visual cortical organization. *Perception* 27:889–935
- Lieberman MC. 1978. Auditory-nerve responses from cats raised in a low-noise chamber. *J. Acoust. Soc. Am.* 63:442–55
- Lieberman P, Blumstein SE. 1988. *Speech Physiology, Speech Perception and Acoustic Phonetics*. New York: Cambridge Univ. Press
- Marr D. 1982. *Vision: A Computational Investigation into the Human Representation and Processing of Visual Information*. San Francisco: Freeman
- Matsubara JA, Phillips DP. 1988. Intracortical connections and their physiological correlates in the primary auditory cortex (AI) in the cat. *J. Comp. Neurol.* 268:38–48
- McMullen NT, de Venicia RK. 1993. Thalamocortical patches in auditory neocortex. *Brain Res.* 620:317–22
- Mendelson JR, Schreiner CE, Sutter ML. 1997. Functional topography of cat primary auditory cortex: response latencies. *J. Comp. Physiol. A* 181:615–34
- Mendelson JR, Schreiner CE, Sutter ML, Grasse K. 1993. Functional topography of cat primary auditory cortex: representation of frequency modulation. *Exp. Brain Res.* 94:65–87
- Merzenich MM, Knight PL, Roth GL. 1975. Representation of the cochlea within primary auditory cortex in the cat. *J. Neurophysiol.* 38:231–49
- Merzenich MM, Reid MD. 1974. Representation of the cochlea within the inferior colliculus of the cat. *Brain Res.* 77:397–415
- Merzenich MM, Schreiner CE. 1992. Mammalian auditory cortex—some comparative observations. In *Evolutionary Biology of Hearing*, ed. AN Popper, DB Webster, RR Fay, pp. 673–89. New York: Springer
- Middlebrooks JC, Dykes RW, Merzenich MM. 1980. Binaural response-specific bands in primary auditory cortex (AI) of the cat: topographical organization orthogonal to isofrequency contours. *Brain Res.* 181:31–48
- Middlebrooks JC, Zook JM. 1983. Intrinsic organization of the cat's medial geniculate body identified by projections to binaural response-specific bands in the primary auditory cortex. *J. Neurosci.* 3:203–24
- Moore BCJ. 1997. *An Introduction to the Psychology of Hearing*. London: Academic
- Nelken I, Prut Y, Vaadia E, Abeles M. 1994a. In search of the best stimulus: an optimization procedure for finding efficient stimuli in the cat auditory cortex. *Hear. Res.* 72:237–53
- Nelken I, Prut Y, Vaadia E, Abeles M. 1994b. Population responses to multifrequency sounds in the cat auditory cortex: one- and two-parameter families of sounds. *Hear. Res.* 72:206–22
- Nelken I, Prut Y, Vaddia E, Abeles M. 1994c. Population responses to multifrequency sounds in the cat auditory cortex: four-tone complexes. *Hear. Res.* 72:223–36
- Nelken I, Rotman Y, Yosef OB. 1999. Responses of auditory-cortex neurons to structural features of natural sounds. *Nature* 397:154–57
- Nienhuys TGW, Clark GM. 1979. Critical bands following the selective destruction of cochlear inner and outer hair cells. *Acta Otolaryngol.* 80:245–54
- Obermayer K, Ritter H, Schulten K. 1990. A principle for the formation of the spatial

- structure of cortical feature maps. *Proc. Natl. Acad. Sci. USA* 87:8345–49
- O'Connor KN, Sutter ML. 1999. Global spectral and location effects in auditory perceptual grouping. *J. Cogn. Neurosci.* In press
- Oliver DL, Morest DK. 1984. The central nucleus of the inferior colliculus of the cat. *J. Comp. Neurol.* 222:237–64
- Oonishi S, Katsuki Y. 1965. Functional organization and integrative mechanism on the auditory cortex of cats. *Jpn. J. Physiol.* 15:342–65
- Patterson RD. 1974. Auditory filter shape. *J. Acoust. Soc. Am.* 55:802–9
- Phillips DP. 1990. Neural representation of sound amplitude in the auditory cortex: effects of noise masking. *Behav. Brain Res.* 37:197–214
- Phillips DP, Hall SE. 1987. Responses of single neurons in cat auditory cortex to time-varying stimuli: linear amplitude modulations. *Exp. Brain Res.* 67:479–92
- Phillips DP, Irvine DR. 1981. Responses of single neurons in physiologically defined primary auditory cortex (AI) of the cat: frequency tuning and responses to intensity. *J. Neurophysiol.* 45:48–58
- Phillips DP, Orman SS. 1984. Responses of single neurons in posterior field of cat auditory cortex to tonal stimulation. *J. Neurophysiol.* 51:147–63
- Phillips DP, Orman SS, Musicant AD, Wilson GF. 1985. Neurons in the cat's primary auditory cortex distinguished by their responses to tones and wide-spectrum noise. *Hear. Res.* 18:73–86
- Phillips DP, Semple MN, Calford MB, Kitzes LM. 1994. Level-dependent representation of stimulus frequency in cat primary auditory cortex. *Exp. Brain Res.* 102:210–26
- Pickles JO. 1975. Normal critical bands in the cat. *Acta Otolaryngol.* 80:245–54
- Plomp R. 1975. *Aspects of Tone Sensation.* London: Academic
- Plomp R, Levelt WJM. 1965. Tonal consonance and critical bandwidth. *J. Acoust. Soc. Am.* 66:1725–32
- Popper AN, Fay RR, eds. 1992. *The Mammalian Auditory Pathway: Neurophysiology.* New York: Springer
- Prieto JJ, Peterson BA, Winer JA. 1994. Morphology and spatial distribution of GABAergic neurons in cat primary auditory cortex (AI). *J. Comp. Neurol.* 344:349–82
- Raggio MW. 1992. *Representation of electrical and acoustic cochlear stimulation in cat primary auditory cortex.* PhD thesis. Univ. Calif, San Francisco. 260 pp.
- Raggio MW, Schreiner CE. 1999. Neuronal responses in cat primary auditory cortex to electrical cochlear stimulation. III: Activation patterns in long- and short-term deafness. *J. Neurophysiol.* In press
- Rauschecker JP. 1998. Parallel processing in the auditory cortex of primates. *Audiol. Neurootol.* 3:86–103
- Rauschecker JP, Tian B, Hauser M. 1995. Processing of complex sounds in the macaque nonprimary auditory cortex. *Science* 268:111–14
- Read HL, Miller LM, Escabi MA, Winer JA, Schreiner CE. 1998. Functionally dynamic isofrequency and non-iso-frequency convergence in cat auditory cortex. *Soc. Neurosci. Abstr.* 24:1878
- Read L, Nauen DW, Larue DT, Schreiner CE, Winer JA. 1999. Do thalamocortical projections engender cochlear magnification changes across the isofrequency axis in cat primary auditory cortex (AI)? *Assoc. Res. Otolaryngol. Abstr.* 22:49
- Reale RA, Imig TJ. 1980. Tonotopic organization in auditory cortex of the cat. *J. Comp. Neurol.* 192:265–91
- Recanzone G, et al. 1999. Functional organization of owl monkey primary auditory cortex. *J. Comp. Neurol.* In press
- Rhode WS, Smith PH. 1985. Characteristics of tone-pip response pattern in relationship to spontaneous rate in cat auditory nerve fibers. *Hear. Res.* 18:159–68
- Rodrigues-Dagaëff C, Simm G, de Ribaupierre Y, Villa A, de Ribaupierre F, Rouiller EM. 1989. Functional organization of the ventral division of the medial geniculate body of

- the cat: evidence for a rostro-caudal gradient of response properties and cortical projections. *Hear. Res.* 39:103–26
- Rouiller EM, Simm G, Villa AEP, de Ribaupierre Y, de Ribaupierre F. 1991. Auditory corticocortical connections in the cat: support for parallel and hierarchical arrangement of the auditory cortical areas. *Exp. Brain Res.* 86:483–505
- Scharf B. 1970. Critical bands. In *Foundations of Modern Auditory Theory*, ed. JV Tobias, 1:159–202. New York: Academic
- Schreiner CE. 1995. Order and disorder in auditory cortical maps. *Curr. Opin. Neurobiol.* 5:489–96
- Schreiner CE. 1998. Spatial distribution of responses to simple and complex sounds in primary auditory cortex. *Audiol. Neurootol.* 3:104–22
- Schreiner CE, Calhoun BM. 1994. Spectral envelope coding in cat primary auditory cortex: properties of ripple transfer functions. *Audit. Neurosci.* 1:39–61
- Schreiner CE, Cynader MS. 1984. Basic functional organization of second auditory cortical field (AII) of the cat. *J. Neurophysiol.* 51:1284–305
- Schreiner CE, Langner G. 1988a. Periodicity coding in the inferior colliculus of the cat. II. Topographic organization. *J. Neurophysiol.* 60:1823–40
- Schreiner CE, Langner G. 1988b. Coding of temporal patterns in the central auditory nervous system. In *Auditory Function*, ed. GM Edelman, WE Gall, M Cowan, pp. 337–61. New York: Wiley
- Schreiner CE, Langner G. 1997. Laminar fine structure of frequency organization in auditory midbrain. *Nature* 388:383–86
- Schreiner CE, Mendelson JR. 1990. Functional topography of cat primary auditory cortex: distribution of integrated excitation. *J. Neurophysiol.* 64:1442–59
- Schreiner CE, Mendelson JR, Sutter ML. 1992. Functional topography of cat primary auditory cortex: representation of tone intensity. *Exp. Brain Res.* 92:105–22
- Schreiner CE, Sutter ML. 1992. Topography of excitatory bandwidth in cat primary auditory cortex: single-neuron versus multiple-neuron recordings. *J. Neurophysiol.* 68:1487–502
- Semple MN, Aitkin LM. 1979. Representation of sound frequency and laterality by units in central nucleus of cat inferior colliculus. *J. Neurophysiol.* 42:1626–39
- Shamma SA, Fleshman JW, Wiser PR, Versnel H. 1993. Organization of response areas in ferret primary auditory cortex. *J. Neurophysiol.* 69:367–83
- Shamma SA, Versnel H. 1995. Ripple analysis in ferret primary auditory cortex. II. Prediction of unit responses to arbitrary spectral profiles. *Audit. Neurosci.* 1:255–70
- Shamma SA, Versnel H, Kowalski N. 1995. Ripple analysis in ferret primary auditory cortex. I. Response characteristics of single units to sinusoidally rippled spectra. *Audit. Neurosci.* 1:233–54
- Shneiderman A, Oliver DL. 1989. EM autoradiography study of the projections from the dorsal nucleus of the lateral lemniscus: a possible source of inhibitory inputs to the inferior colliculus. *J. Comp. Neurol.* 286:28–47
- Suga N. 1977. Amplitude-spectrum representation in the Doppler-shift processing area of the auditory cortex of the mustached bat. *Science* 196:64–67
- Suga N. 1984. The extent to which biosonar information is represented in the bat auditory cortex. In *Dynamic Aspects of Neocortical Function*, ed. GM Edelman, WE Gall, WM Cowan, pp. 315–73. New York: Wiley
- Suga N. 1995. Sharpening of frequency tuning by inhibition in the central auditory system: tribute to Yasuji Katsuki. *Neurosci. Res.* 21:287–99
- Suga N, Manabe T. 1982. Neural basis of amplitude-spectrum representation in auditory cortex of the mustached bat. *J. Neurophysiol.* 47:225–55
- Suga N, Tsuzuki K. 1985. Inhibition and level-tolerant frequency tuning in the auditory cortex of the mustached bat. *J. Neurophysiol.* 53:1109–45

- Suga N, Zhang Y, Yan J. 1997. Sharpening of frequency tuning by inhibition in the thalamic auditory nucleus of the mustached bat. *J. Neurophysiol.* 77:2098–114
- Sutter ML, Schreiner CE. 1991. Physiology and topography of neurons with multi-peaked tuning curves in cat primary auditory cortex. *J. Neurophysiol.* 65:1207–26
- Sutter ML, Schreiner CE. 1995. Topography of intensity tuning in cat primary auditory cortex: single-neuron versus multiple-neuron recordings. *J. Neurophysiol.* 73:190–204
- Sutter ML, Schreiner CE, McLean M, O'Connor KN, Loftus WC. 1999. Organization of frequency receptive fields in cat AI. *J. Neurophysiol.* In press
- Taha S, Bonham B, Wong SW, Schreiner CE. 1996. Intra-cortical inhibitory connections refine the specificity of cat AI neuron responsiveness. *Soc. Neurosci. Abstr.* 22:465
- Versnel H, Kowalski N, Shamma SA. 1995. Ripple analysis in ferret primary auditory cortex. III. Topographic distribution of ripple response parameters. *Audit. Neurosci.* 1:271–85
- Wallace MN, Kitzes LM, Jones EG. 1991. Intrinsic inter- and intralaminar connections and their relationship to the tonotopic map in cat primary auditory cortex. *Exp. Brain Res.* 86:527–44
- Wang J, Salvi RJ, Caspary DM, Powers N. 1996. GABAergic inhibition profoundly alters the tuning and discharge rate of neurons in the primary auditory cortex of the chinchilla. *Assoc. Res. Otolaryngol. Abstr.* 19:156
- Wang K, Shamma SA. 1995. Spectral shape analysis in the central auditory system. *IEEE Transact. Speech Audio Proc.* 3:382–95
- Wang X, Beitel RE, Schreiner CE, Merzenich MM. 1995. Systematic distribution of response latencies along the isofrequency axis of monkey primary auditory cortex. *Soc. Neurosci. Abstr.* 21:669
- Wenstrup JJ, Grose CD. 1995. Inputs to combination-sensitive neurons in the medial geniculate body of the mustached bat: the missing fundamental. *J. Neurosci.* 15:4693–711
- Winer JA. 1992. The functional architecture of the medial geniculate body and the primary auditory cortex. See Popper & Fay, pp. 222–409
- Zipser K, Lamme VA, Schiller PH. 1996. Contextual modulation in primary visual cortex. *J. Neurosci.* 16:7376–89
- Zwicker E, Flottrop G, Stevens SS. 1957. Critical band width in loudness summation. *J. Acoust. Soc. Am.* 29:548–57

